Performance Analysis of Equalized OFDM Systems in Rayleigh Fading

Ming-Xian Chang, and Yu T. Su, *Member, IEEE*

***Abstract*—Channel estimation is usually needed to compensate for the amplitude and phase distortions associated with a received orthogonal frequency-division multiplexing (OFDM) waveform. This paper presents a systematic approach for analyzing the bit-error probability (BEP) of equalized OFDM signals in Rayleigh fading. Closed-form expressions for BEP performance of various signal constellations [phase-shift keying (PSK), differential phase-shift keying (DPSSK), quaternary phase-shift keying (QPSK)] are provided for receivers that use a linear pilot-assisted channel estimate. We also derive the optimal linear channel estimates that yield the minimum BEP and show that some previous known results are special cases of our general formulae. The results obtained here can be applied to evaluate the performance of equalized single-carrier narrowband systems as well.**

***Index Terms*—Error analysis, frequency division multiplexing, gain control.**

I. Introduction

ORTHOGONAL frequency-division multiplexing (OFDM) is a promising candidate technique for high speed transmissions in a frequency-selective fading environment [1]. By converting a wideband signal into an array of properly-spaced narrowband signals for parallel transmission, each narrowband OFDM signal suffers from frequency-flat fading and, thus, needs only a one-tap equalizer to compensate for the corresponding multiplicative channel distortion.

One popular method to estimate the multiplicative channel response (CR) is to insert pilot symbols among transmitted data symbols [2]–[9]. Though many pilot-assisted channel estimation algorithms have been suggested, there still lacks a general analysis for the associated bit-error probability (BEP) performance. This paper presents a systematic approach for evaluating the BEP performance of OFDM receivers in Rayleigh fading when a linear pilot-assisted channel estimate is used. These BEP expressions are functions of the average bit signal energy to noise level ratio (SNR), $\overline{\gamma}_b \triangleq \overline{E}_b/N_0$ and some correlation coefficients that depend on the true channel statistic and the estimation method used. Our derivations are based on the facts that Rayleigh fading is resulted from a zero-mean complex Gaussian CR process and a linear pilot-assisted channel estimate is a linear function of the true CRs at pilot symbol locations. Using our general result, we are able to derive the optimal linear channel estimate that provides the best BEP performance.

The rest of this paper is organized as follows. Section II provides a mathematical model of an OFDM system in Rayleigh fading and gives a brief descriptions of some CR estimation algorithms. Section III contains our BEP analysis for phase-shift keying (PSK), differential PSK (DPSK) and quadrature amplitude modulation (QAM) constellations while Section IV deals with the BEP performance for general linear channel estimates. Section V gives some numerical examples based on our analysis. Finally, Section VI summarizes our main results.

Manuscript received September 18, 2001; revised November 20, 2001; accepted March 31, 2002. The editor coordinating the review of this paper and approving it for publication is Y.-C. Liang. This work was supported in part by the MOE Program of Excellence under Grant 89-E-FA06-2-4 and National Science Council of Taiwan under Grant NSC86-2221-E-009-058. Part of this work was presented at the IEEE VTC'2000, May 2000, Tokyo, Japan.

M.-X. Chang was with the Department of Communication Engineering, National Chiao Tung University, Hsinchu 30056, Taiwan. He is now with the Department of Electrical Engineering, National Cheng Kung University, Tainan, Taiwan (e-mail: mxc@ncku.edu.tw).

Y. T. Su is with the Department of Communication Engineering, National Chiao Tung University, Hsinchu 30056, Taiwan (e-mail: ytsu@cc.nctu.edu.tw).

Digital Object Identifier 10.1109/TWC.2002.804181

II. System Model and Channel Estimate Algorithms

A. Signal and Channel Models

A baseband OFDM signal during the nth symbol interval can be expressed by

$$x(t) = \sum_{m=0}^{N_c-1} X_{mn} \exp\left(\frac{i2\pi mt}{T}\right),\ (n-1)T \le t < nT \quad (1)$$

where N_c denotes the number of narrowband channels, $\omega_m = 2\pi m/T$, T being a symbol duration and X_{mn} represents the data symbol of the mth subchannel in the nth time interval. The values X_{mn} assumes depend on the signal constellation format. For example, quaternary phase-shift keying (QPSK) is represented by the set $\{a+ib|a,b \in (\pm 1)\}$ while the rectangular 16-QAM is the set $\{a+ib|a,b \in (\pm 1, \pm 3)\}$. The corresponding sampled version of $x(t)$ is equal to the inverse discrete Fourier transform (IDFT) of $\{X_{mn}\}_{m=0}^{N_c-1}$, i.e.

$$x_{k,n} = x(t)|_{t=(n-1)T+kT/N_c} = \sum_{m=0}^{N_c-1} X_{mn} e^{i2\pi mk/N_c}. \quad (2)$$

A guard time of $T_g\ (\ll T)$ s is usually inserted such that the resulting waveform during the nth "extended" symbol interval becomes (3), shown at the bottom of the next page, where $T_s = T_g + T$. $x_g(t)$ is further modified by a pulse shaping filter, yielding a transmitted baseband waveform that can be expressed as $x_g(t)p(t)$, where $p(t)$ is of duration T_s and unit power. The corresponding received baseband signal is then given by

$$z(t) = \sum_{j=1}^{N_p} h_j(t) x_g\left(t-\tau_j(t)\right) p\left(t-\tau_j(t)\right) + \sqrt{2}\, n(t) \quad (4)$$

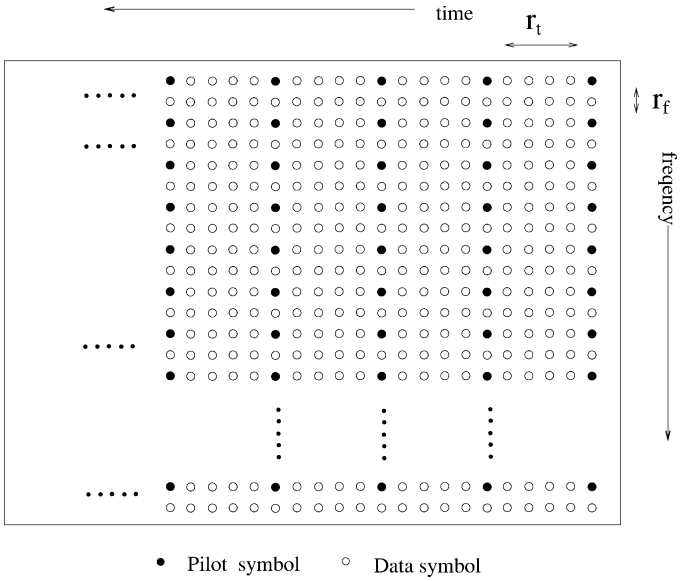

Fig. 1. A typical pilot symbol distribution in the time-frequency plane of an OFDM system. r_t and r_f are the numbers of data symbols between two neighboring pilot symbols in the time and frequency domains, respectively. The parameter values for this distribution are $r_t = 4$ and $r_f = 1$.

where N_p is the number of paths of the channel, $\tau_j(t)$ and $h_j(t)$ are the the delay and the complex fading envelope of the jth path and $n(t) = n_c(t) + in_s(t)$, $n_c(t)$ and $n_s(t)$ being independent lowpass white Gaussian noise processes with the same flat spectral density $N_0/2$ (W/Hz).

$z(t)$ is filtered by a matched filter and sampled at N_c/T samples/second. Removing those samples in guard intervals and performing DFT on $\{y_k\}$, we obtain

$$Y_{mn} = H_{mn}X_{mn} + N_{mn} \tag{5}$$

where $N_{mn} = N_{I,mn} + iN_{Q,mn}$ is a zero-mean complex Gaussian random variable with independent in-phase and quadrature phase components and identical variance $var(N_I) = var(N_Q) = N_0/2T \triangleq \sigma_n^2$. Furthermore

$$H_{mn} = \sum_{k=1}^{N_p} h_k[n] \exp\left\{\frac{-i2\pi m\tau_k[n]}{T_s}\right\} \tag{6}$$

represents the corresponding channel effect (response).

Equation (5) implies that, if H_{mn} is perfectly known, the maximum-likelihood (ML) receiver would select the signal point in the constellation that is closest to $\hat{X}_{mn} = Y_{mn}/H_{mn}$. When the true CR is not known, the receiver needs a CR estimate $\hat{H}_{mn}$ to make a symbol decision. A practical solution, as mentioned before, is to insert pilot symbols at some predetermined (pilot) locations in the time-frequency plane (see Fig. 1), where the (m, n)th location denotes the mth channel and the nth time interval. Usually, a receiver would first estimate the CRs at pilot locations and then, based on this information, obtain CR estimations at other (data symbols) locations through interpolation.

B. CR Estimates at Pilot Locations

1) The LS Method: One obvious CR estimate at a pilot location (m, n) is the least-squares (LS) estimate [2]

$$\hat{H}_{mn,\mathrm{LS}} = \frac{Y_{mn}}{X_{mn}} = H_{mn} + \frac{N_{mn}}{X_{mn}} = H_{mn} + V_{mn} \tag{7}$$

where V_{mn} is the error term due to the presence of noise N_{mn} whose conditional variance is $E[|V_{mn}|^2 \mid X_{mn}] = 2\sigma_n^2/|X_{mn}|^2$. The corresponding vector representation of (7) is given by

$$\hat{\mathbf{h}}_{LS} = \mathbf{h} + \mathbf{X}^{-1}\mathbf{n} = \mathbf{h} + \mathbf{v} \tag{8}$$

where bold face lowercase letters are vectors of the corresponding terms in (7) and $\mathbf{X}$ is a diagonal matrix with pilot symbols X_{mn}s as its diagonal elements. We shall use bold face uppercase and lowercase letters to denote matrices and vectors throughout our discussion.

2) Linear Minimum Mean-Squared Error (LMMSE) Method: A more elaborate method that is capable of reducing the effect of V_{mn} is the LMMSE method [2]–[5]. Based on the estimated channel autocorrelation matrix $\tilde{\mathbf{R}}_{\mathbf{h}}$ and the noise variance $\tilde{\sigma}_n^2$, this method yields the following CR estimation vector $\hat{\mathbf{h}}_{LMMSE}$ at the pilot locations [3]

$$\hat{\mathbf{h}}_{\mathrm{LMMSE}} = \tilde{\mathbf{R}}_{\mathbf{h}}\left[\tilde{\mathbf{R}}_{\mathbf{h}} + 2\tilde{\sigma}_n^2\left(\mathbf{X}\mathbf{X}^{\mathrm{H}}\right)^{-1}\right]^{-1}\hat{\mathbf{h}}_{LS} \tag{9}$$

where $\mathbf{X}^{\mathrm{H}}$ represents the Hermitian of $\mathbf{X}$.

C. CR Estimates at Data Locations

1) Polynomial Interpolation: After the CRs at pilot locations are obtained, either by the LS or LMMSE method, the CRs at data locations can then be estimated by various interpolation methods [5]. For example, if we have three pilot CR estimates, $\hat{H}_0$, $\hat{H}_L$ and $\hat{H}_{2L}$ of a given subchannel, we need to the find the coefficients of the degree-2 polynomial

$$\hat{H}(n) = c_2n^2 + c_1n + c_0 \tag{10}$$

such that $\hat{H}(0) = \hat{H}_0$, $\hat{H}(L) = \hat{H}_L$ and $\hat{H}(2L) = \hat{H}_{2L}$. The coefficients (c_0, c_1, c_2) can be obtained by solving the Lagrange interpolating polynomial

$$\hat{H}(n) = \frac{(n-L)(n-2L)}{(0-L)(0-2L)}\hat{H}_0 + \frac{(n-0)(n-2L)}{(L-0)(L-2L)}\hat{H}_L + \frac{(n-0)(n-L)}{(2L-0)(2L-L)}\hat{H}_{2L}. \tag{11}$$

2) Model-Based Estimate: The CRs at data locations can also be estimated by applying regression surface model to LS-estimated CRs of pilots [8], [9]. The model-based approach divides the time-frequency plane into blocks of the same basic

$$x_g(t) = \begin{cases} x\left(t - nT_g + T\right), & (n-1)T_s \le t < (n-1)T_s + T_g \\ x\left(t - nT_g\right), & (n-1)T_s + T_g \le t \le nT_s \end{cases} \tag{3}$$

structure and finds a nonlinear two-dimensional surface that best fits the CRs of the pilot locations within a block. The noise effect of LS-estimated pilot CRs is greatly reduced by this solution. Furthermore, this approach does not need channel information such as the channel autocorrelation matrix and the noise level N_0.

3) General Linear CR Estimate: Although estimating the CRs at data locations may involve a nonlinear interpolating polynomial, e.g., (10), the derived data CR estimate, e.g., (11), is still a linear combinations of LS- or LMMSE-estimated pilot CRs. Since each LMMSE-estimated pilot CR is also a linear function of the LS-estimated pilot CRs [see (9)], the resulting data CR estimate is a linear function of the LS-estimated pilot CRs. This conclusion is also valid for the model-based CR estimate [8], [9] and other modified algorithms based on the LS or LMMSE method. In summary, for a general class of linear channel estimates, we can express the CR estimate as

$$\hat{H} = \mathbf{a}^{\mathrm{H}}\hat{\mathbf{h}}_{LS} = \mathbf{a}^{\mathrm{H}}(\mathbf{h}+\mathbf{v}) = \mathbf{a}^{\mathrm{H}}\mathbf{h} + W = H' + W \quad (12)$$

where $W = \mathbf{a}^{\mathrm{H}}\mathbf{v}$ is the noise component in $\hat{H}$ and $H' = \mathbf{a}^{\mathrm{H}}\mathbf{h}$ can be viewed as the channel estimate in the absence of noise. The weighting vector $\mathbf{a}$ is a function of both the pilot CR estimation algorithm and the interpolation method.

III. BEP Analysis

Throughout our analysis, we shall assume that the true CR, H_{mn}, is a bandpass wide sense stationary zero-mean complex Gaussian process so that at a given location, (m,n), $|H_{mn}|$ is Rayleigh distributed and $\angle H_{mn}$ is uniformly distributed within $[-\pi,\pi)$. We begin with BEP analysis for systems with a channel estimate that can also be modeled as a bandpass stationary zero-mean complex Gaussian process. Dropping the time and frequency indices for convenience, we have

$$Y = HX + N, \quad H \triangleq x_1 + ix_2 = r_1 e^{i\phi_1} \quad (13)$$

$$\hat{H} = H' + W \triangleq x_3 + ix_4 = r_2 e^{i\phi_2} \quad (14)$$

where H is the true CR and $\hat{H}$ is the estimated CR. The equation $\hat{H} = H' + W$, as can be seen from (12), decomposes $\hat{H}$ into the noise-absent estimate H' and the noise component W. The additive white Gaussian noise (AWGN) N is complex Gaussian distributed with zero mean and variance $E[|N|^2] = 2\sigma_n^2$. Because W is a function of noise samples at pilot locations while N is the noise component at a data symbol location, W is independent of N. On the other hand, $\hat{H}$ is a linear combination of LS-estimated CRs, which, as can be seen from (7), are complex Gaussian distributed, it is also complex Gaussian distributed. We, therefore, conclude that x_1, x_2, x_3 and x_4 are all Gaussian distributed, r_1 and r_2 are Rayleigh distributed and ϕ_1 and ϕ_2 are uniformly distributed in $[-\pi,\pi)$.

Invoking the general Rayleigh fading process assumption, x_1, x_2 are independent and identically distributed (i.i.d.) processes with

$$E\left[x_1^2\right] = E\left[x_2^2\right] = \frac{1}{2}E\left[|H|^2\right] \triangleq \sigma_1^2,\ E[x_1x_2] = 0 \quad (15)$$

we can show that x_3, x_4 are also i.i.d. processes (see Appendix A) with

$$E\left[x_3^2\right] = E\left[x_4^2\right] = \frac{1}{2}E\left[|\hat{H}|^2\right] \triangleq \sigma_2^2 \quad (16)$$

$$E[x_3x_4] = 0 \quad (17)$$

$$E[x_1x_3] = E[x_2x_4] = \frac{1}{2}\mathrm{Re}\left\{E\left[\hat{H}H^*\right]\right\} \triangleq \mu_1 \quad (18)$$

$$E[x_1x_4] = -E[x_2x_3] = \frac{1}{2}\mathrm{Im}\left\{E\left[\hat{H}H^*\right]\right\} \triangleq \mu_2. \quad (19)$$

The correlation coefficients and average SNR per bit are defined, respectively, as

$$\rho_1 \triangleq \frac{\mu_1}{\sigma_1\sigma_2}, \quad \rho_2 \triangleq \frac{\mu_2}{\sigma_1\sigma_2}, \quad \rho \triangleq \sqrt{\rho_1^2+\rho_2^2} \quad (20)$$

$$\overline{\gamma}_b \triangleq \frac{E\left[|HX|^2\right]}{KE\left[|N|^2\right]} = \frac{E\left[|H|^2\right]E\left[|X|^2\right]}{KE\left[|N|\right]^2} = \frac{2\sigma_1^2\,E\left[|X|^2\right]}{2\sigma_n^2K} \quad (21)$$

where K denotes the number of bits represented by one symbol. For example, $K=2$ for QPSK, $K=4$ for 16-QAM.

Note that (18) and (19) imply

$$\frac{1}{2}E\left[\hat{H}H^*\right] = \mu_1 + i\mu_2 \quad (22)$$

and for a reasonably good estimate, i.e., $\hat{H} \approx H$, (22) then leads to $E[\hat{H}H^*] \approx E[|H|^2]$ and $\mu_2 \approx 0$ ($\rho_2 \approx 0$). Furthermore, the mean-squared estimation error (MSEE) is

$$E\left[\left|\hat{H}-H\right|^2\right] = 2\left(\sigma_1^2+\sigma_2^2-2\mu_1\right) \quad (23)$$

which is independent of μ_2 (ρ_2). However, as we will see shortly that the BEP performance of systems with imperfect channel estimate does indeed depend on ρ_2 (μ_2). Hence, the MSEE, as a performance measure, is not necessarily proper in general. An exception can be found in single-carrier narrowband channels based on Jakes or similar models in which we have $\rho_2 = \mu_2 = 0$; see (66).

The joint probability density function (pdf) of (x_1,x_2,x_3,x_4) [11] is given by (24), shown at the bottom of the page. Transforming the rectangular coordinate (x_1,x_2,x_3,x_4) into the

$$p(x_1,x_2,x_3,x_4) = \frac{1}{(2\pi)^2\left(\sigma_1^2\sigma_2^2-\mu_1^2-\mu_2^2\right)}\exp\left[-\frac{\sigma_2^2\left(x_1^2+x_2^2\right)+\sigma_1^2\left(x_3^2+x_4^2\right)-2\mu_1(x_1x_3+x_2x_4)-2\mu_2\left(x_1x_4-x_2x_3\right)}{2\left(\sigma_1^2\sigma_2^2-\mu_1\mu_2\right)}\right]. \quad (24)$$

polar coordinate $(r_1, r_2, \phi_1, \phi_2)$ and making the changes of variables, $\psi = \phi_1 - \phi_2$, we have $p(r_1, r_2, \psi)$ in (25).

$$p(r_1, r_2, \psi) = \frac{r_1 r_2}{2\pi\sigma_1^2\sigma_2^2(1-\rho^2)} \exp\left\{-\frac{1}{2(1-\rho^2)} \cdot \left[\frac{r_1^2}{\sigma_1^2} + \frac{r_2^2}{\sigma_2^2} - 2\frac{r_1 r_2}{\sigma_1\sigma_2}(\rho_1\cos\psi - \rho_2\sin\psi)\right]\right\}. \quad (25)$$

The parameters ρ_1, ρ_2, and σ_2 in (25) are functions of the channel statistic and the CR estimation method used. More detailed expressions for them will be given in Section IV-A.

Expressing an equalized symbol $\hat{X} = Y/\hat{H}$ as

$$\begin{aligned}\hat{X} =& \frac{HX+N}{\hat{H}} \\ =& \frac{1}{\left|\hat{H}\right|}\left(|H|e^{i(\angle H - \angle\hat{H})}X + |N|e^{i(\angle N - \angle\hat{H})}\right) \\ =& \frac{1}{\left|\hat{H}\right|}\left(|H|e^{i\psi}X + N'\right)\end{aligned} \quad (26)$$

we notice that $N' = Ne^{-i\angle\hat{H}}$ is a zero-mean complex Gaussian random variable whose variance is the same as that of N. It can be shown that N' is also independent of W even though the phase-shift $\angle\hat{H}$ and W are correlated. Using (13) and (14), we can rewrite (26) as

$$\hat{X} = \frac{1}{r_2}\left(r_1 e^{i\psi}X + N'\right). \quad (27)$$

A. Binary Phase Shift Keying (BPSK) and QPSK Systems

Coherent BPSK and QPSK receivers base their symbol decisions solely on the phase location of the associated matched filter output. Equation (27) indicates that such decisions are independent of $|\hat{H}| = r_2$. Their respective BEPs conditioned on a fixed phase error ψ and fading envelope $r_1(= |H|)$ are given in [15, 10.14a]

$$P_b(E|\psi, r_1) = Q\left(\frac{r_1}{\sigma_n}\cos\psi\right) \quad (28)$$

for BPSK and

$$P_b(E|\psi, r_1) = \frac{1}{2}Q\left(\frac{r_1}{\sigma_n}[\cos\psi - \sin\psi]\right) + \frac{1}{2}Q\left(\frac{r_1}{\sigma_n}[\cos\psi + \sin\psi]\right) \quad (29)$$

for QPSK, where $Q(x) \triangleq 1/\sqrt{2\pi}\int_x^\infty e^{-t^2/2}dt$. We can express the (unconditional) BEPs in a Rayleigh fading channel as

$$P_b(E) = \int_0^\infty\int_0^\infty\int_{-\pi}^{\pi} P_b(E|\psi, r_1)\, p(r_1, r_2, \psi)\, d\psi dr_1 dr_2. \quad (30)$$

Substituting (25), (28), and (29) into (30) and using the integral formula (B.1) of Appendix B, we obtain

$$P_b(E) = \frac{1}{2}\left[1 - \frac{\rho_1}{\sqrt{1 + \frac{1}{\overline{\gamma}_b} - \rho_2^2}}\right] \quad (31)$$

for an OFDM-BPSK system and

$$P_b(E) = \frac{1}{2}\left[1 - \frac{1}{2}\frac{\frac{(\rho_1+\rho_2)}{\sqrt{2}}}{\sqrt{1 + \frac{1}{2\overline{\gamma}_b} - \frac{(\rho_1-\rho_2)^2}{2}}} - \frac{1}{2}\frac{\frac{(\rho_1-\rho_2)}{\sqrt{2}}}{\sqrt{1 + \frac{1}{2\overline{\gamma}_b} - \frac{(\rho_1+\rho_2)^2}{2}}}\right] \quad (32)$$

for an OFDM-QPSK system. In the above two equations, (31) and (32)

$$\overline{\gamma}_b = \frac{2\sigma_1^2}{(2\sigma_n^2)} \quad (33)$$

is the average SNR per bit for both BPSK and QPSK systems, as can be seen from (21).

B. DPSK System (Without Channel Equalization)

The need of channel equalization can be avoided by using DPSK modulation if the difference of channel-induced phase rotation remains relatively small during two or more symbol intervals. The performance of a narrowband DPSK or an OFDM-DPSK system can also be analyzed by the same method presented in the above subsection. Neglecting the subscript denoting the channel number and leaving only the time index, we have

$$\begin{aligned}\frac{Y_n}{Y_{n-1}} =& \frac{H_n X_n + N_n}{H_{n-1}X_{n-1} + N_{n-1}} \\ =& \frac{1}{H_{n-1} + \frac{N_{n-1}}{X_{n-1}}}\left(H_n\frac{X_n}{X_{n-1}} + \frac{N_n}{X_{n-1}}\right) \\ =& \frac{1}{\left|H_{n-1} + \frac{N_{n-1}}{X_{n-1}}\right|}\left(|H_n|\, e^{i\psi}\frac{X_n}{X_{n-1}} + \frac{N_n'}{|X_{n-1}|}\right)\end{aligned} \quad (34)$$

where the phase of X_n/X_{n-1} contains the data information of a DPSK signal. The parameter ψ now represents the phase difference between H_n and the pseudo CR estimate $\hat{H}_n = H_{n-1} + N_{n-1}/X_{n-1}$. Comparing (34) with (26) and assuming a Jakes Rayleigh channel [14], we obtain, from the definitions given by (15)–(21),

$$\sigma_1^2 = \frac{E\left[|H_n|^2\right]}{2} \quad (35)$$

$$\sigma_2^2 = \frac{E\left[\left|\hat{H}_n\right|^2\right]}{2} = \frac{\sigma_1^2 + \sigma_n^2}{|X|^2} \quad (36)$$

$$\mu_1 + i\mu_2 = \frac{1}{2}E\left[H_n H_{n-1}^*\right] = \sigma_1^2 J_0(2\pi f_d T_s) \quad (37)$$

$$\rho_1 = \frac{\mu_1}{\sigma_1\sigma_2} = \frac{J_0(2\pi f_d T_s)}{\sqrt{1 + \frac{1}{|X|^2\overline{\gamma}_b}}} \quad (38)$$

$$\rho_2 = \frac{\mu_2}{\sigma_1\sigma_2} = 0 \quad (39)$$

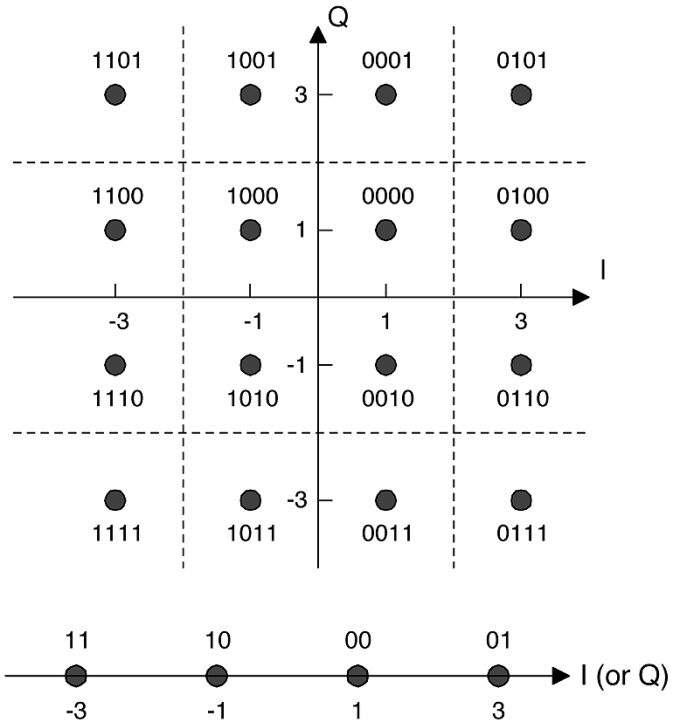

Fig. 2. Constellation of Gray-coded rectangular 16-QAM and the corresponding I-Q bit mapping.

where H_{n-1}^{*} denotes the complex conjugate of H_{n-1}. Substituting ρ_1 and ρ_2 into (31) and (32) we have, for differential BPSK ($|X|^2 = 1$),

$$P_b(E) = \frac{1}{2}\left[1 - \frac{J_0(2\pi f_d T_s)}{1+\frac{1}{\bar{\gamma}_b}}\right] \tag{40}$$

which is the same as (13-34) of [13] and, for differential QPSK ($|X|^2 = 2$)

$$P_b(E) = \frac{1}{2}\left(1 - \frac{J_0(2\pi f_d T_s)}{\sqrt{\left(2+\frac{1}{\bar{\gamma}_b}\right)\left(1+\frac{1}{2\bar{\gamma}_b}\right) - J_0(2\pi f_d T_s)}}\right). \tag{41}$$

Note that for slow fading (zero or very small Doppler) channels, $J_0(\cdot) \approx 1$, (40) then becomes

$$P_b(E) = \frac{1}{2}\left(1 - \frac{1}{1+\frac{1}{\bar{\gamma}_b}}\right) \tag{42}$$

while (41) is reduced to

$$P_b(E) = \frac{1}{2}\left(1 - \frac{1}{\sqrt{1+\frac{2}{\bar{\gamma}_b}+\frac{1}{2\bar{\gamma}_b^2}}}\right) \tag{43}$$

which coincides with (50b) of [16].

C. QAM Systems

This subsection gives the BEP performance analysis of the rectangular 16-QAM constellation with gray-bit mapping shown in Fig. 2. The performance of other QAM constellations, like rectangular 64-QAM or 128-QAM, can be derived in a similar manner. Unlike PSK or DPSK signals, the performance of QAM systems does depend on the the distribution of $|\hat{H}| = r_2$.

A 16-QAM symbol can be written as $X = X_i + iX_q = |X|e^{i\theta}$, where X_I, $X_Q \in \{1, -1, 3, -3\}$. From (27), we have the equalized data symbol

$$\begin{aligned}\hat{X} =& \frac{1}{r_2}\left(r_1|X|e^{i(\theta+\psi)} + N'\right)\\ =& \frac{r_1|X|\cos(\theta+\psi)+N_I}{r_2} + i\frac{r_1|X|\sin(\theta+\psi)+N_Q}{r_2}\\ =& \hat{X}_I + i\hat{X}_Q\end{aligned} \tag{44}$$

where $N' = N_I + iN_Q$. If the transmitted symbol is, say, $X = 1 + i3$, then the corresponding bit pattern is 0001 with I and Q components being 00 and 01, respectively. The conditional BEPs for the component channels are thus, given by

$$\begin{aligned}P_{b,I}(E|r_1, r_2, \psi, 0001) =& \frac{1}{2}\Pr\left(\hat{X}_I > 2\,|X_I = 1\right)\\ &+ \frac{1}{2}\Pr\left(\hat{X}_I < 0\,|X_I = 1\right)\\ &+ \frac{1}{2}\Pr\left(\hat{X}_I < -2\,|X_I = 1\right)\end{aligned} \tag{45}$$

$$\begin{aligned}P_{b,Q}(E|r_1, r_2, \psi, 0001) =& \frac{1}{2}\Pr\left(\hat{X}_Q < 2\,|X_Q = 3\right)\\ &+ \frac{1}{2}\Pr\left(\hat{X}_Q < 0\,|X_Q = 3\right)\\ &- \frac{1}{2}\Pr\left(\hat{X}_Q < -2\,|X_Q = 3\right).\end{aligned} \tag{46}$$

The above equations, (44)–(46) lead to

$$\begin{aligned}&P_b(E|r_1, r_2, \psi, 0001)\\ &=\frac{1}{2}P_{b,I}(E|r_1, r_2, \psi, 0001) + \frac{1}{2}P_{b,Q}(E|r_1, r_2, \psi, 0001)\\ &=\frac{1}{4}\Pr\left(\frac{r_1|X|\cos(\theta+\psi)+N_I}{r_2} > 2\right)\\ &\quad+\frac{1}{4}\Pr\left(\frac{r_1|X|\cos(\theta+\psi)+N_I}{r_2} < 0\right)\\ &\quad+\frac{1}{4}\Pr\left(\frac{r_1|X|\cos(\theta+\psi)+N_I}{r_2} < -2\right)\\ &\quad+\frac{1}{4}\Pr\left(\frac{r_1|X|\sin(\theta+\psi)+N_Q}{r_2} < 2\right)\\ &\quad+\frac{1}{4}\Pr\left(\frac{r_1|X|\sin(\theta+\psi)+N_Q}{r_2} < 0\right)\\ &\quad-\frac{1}{4}\Pr\left(\frac{r_1|X|\sin(\theta+\psi)+N_Q}{r_2} < -2\right)\\ &=\frac{1}{4}\Pr\left(N_I > 2r_2 - r_1|X|\cos(\theta+\psi)\right)\\ &\quad+\frac{1}{4}\Pr\left(-N_I > r_1|X|\cos(\theta+\psi)\right)\\ &\quad+\frac{1}{4}\Pr\left(-N_I > 2r_2 + r_1|X|\cos(\theta+\psi)\right)\\ &\quad+\frac{1}{4}\Pr\left(-N_Q > -2r_2 + r_1|X|\sin(\theta+\psi)\right)\\ &\quad+\frac{1}{4}\Pr\left(-N_Q > r_1|X|\sin(\theta+\psi)\right)\\ &\quad-\frac{1}{4}\Pr\left(-N_Q > 2r_2 + r_1|X|\sin(\theta+\psi)\right)\end{aligned} \tag{47}$$

where $X = 1+i3$. We can obtain the conditional BEPs of other transmitted bit patterns

$$P_b\left(E|r_1, r_2, \psi, d_0d_1d_2d_3\right), \quad d_k \in \{0,1\}$$

in a similar manner and the overall conditional BEP is

$$P_b\left(E|r_1, r_2, \psi\right) = \sum_{(d_0d_1d_2d_3)} \frac{1}{16} P_b\left(E|r_1, r_2, \psi,\, d_0d_1d_2d_3\right) \tag{48}$$

where each term on the right hand side is either of the form

$$\begin{aligned}\Pr\left[\pm N_{I(Q)} > a\cdot r_2 + b\cdot r_1\cos(\psi+\theta)\right] \\ = Q\left(\frac{a\cdot r_2 + b\cdot r_1\cos(\psi+\theta)}{\sigma_n}\right)\end{aligned} \tag{49}$$

or

$$\begin{aligned}\Pr\left[\pm N_{I(Q)} > a\cdot r_2 + b\cdot r_1\sin(\psi+\theta)\right] \\ = Q\left(\frac{a\cdot r_2 + b\cdot r_1\sin(\psi+\theta)}{\sigma_n}\right)\end{aligned} \tag{50}$$

with $a \in \{0, \pm 2\}$, $b = \pm|X| = \pm\sqrt{X_I^2 + X_Q^2} \in \{\pm\sqrt{2}, \pm\sqrt{10}, \pm\sqrt{18}\}$. As in (30), the BEP is given by

$$\begin{aligned}P_b(E) = \int_0^\infty \int_0^\infty \int_{-\pi}^{\pi} P_b\left(E|r_1, r_2, \psi\right) \\ \cdot p\left(r_1, r_2, \psi\right) d\psi dr_1 dr_2.\end{aligned} \tag{51}$$

For the rectangular 16-QAM, the average SNR per bit defined by (21) becomes

$$\overline{\gamma}_b = \frac{5}{2}\frac{\sigma_1^2}{\sigma_n^2}. \tag{52}$$

Substituting (25), (48), and (52) into (51) and using (B.1) in Appendix B, we obtain (53) shown at the bottom of the page, where the associated coefficients $(\text{sgn}_k, a_k, b_k, \cos\theta_k, \sin\theta_k)$ are listed in in Table I.

The BEP expression of the 16-QAM system in flat Rayleigh fading derived in [10] involves a few finite-range integrals. Using the above equation with $\rho_2 = 0$, $\rho_1 = \rho$, we can obtain a closed-form expression instead.

IV. Performance of General Linear Channel Estimates

As discussed in Section II-B, a linear pilot-assisted CR estimate can be written as

$$\hat{H} = \mathbf{a}^{\mathrm{H}}\hat{\mathbf{h}}_{LS} = \mathbf{a}^{\mathrm{H}}(\mathbf{h}+\mathbf{v}) = \mathbf{a}^{\mathrm{H}}\left(\mathbf{h}+\mathbf{X}^{-1}\mathbf{n}\right) = H' + W \tag{54}$$

TABLE I
Coefficients Associated With Various Terms in (53)

k	sgn_k	a_k	b_k	$\cos(\theta_k)$	$\sin(\theta_k)$
1	+	2	$-\sqrt{2}$	$1/\sqrt{2}$	$1/\sqrt{2}$
2	+	0	$\sqrt{2}$		
3	+	2	$\sqrt{2}$		
4	+	2	$-\sqrt{2}$	$1/\sqrt{2}$	$-1/\sqrt{2}$
5	+	0	$\sqrt{2}$		
6	+	2	$\sqrt{2}$		
7	+	2	$-\sqrt{10}$	$1/\sqrt{10}$	$3/\sqrt{10}$
8	+	0	$\sqrt{10}$		
9	+	2	$\sqrt{10}$		
10	+	-2	$\sqrt{10}$	$3/\sqrt{10}$	$-1/\sqrt{10}$
11	+	0	$\sqrt{10}$		
12	-	2	$\sqrt{10}$		
13	+	-2	$\sqrt{10}$	$3/\sqrt{10}$	$1/\sqrt{10}$
14	+	0	$\sqrt{10}$		
15	-	2	$\sqrt{10}$		
16	+	2	$-\sqrt{10}$	$1/\sqrt{10}$	$-3/\sqrt{10}$
17	+	0	$\sqrt{10}$		
18	+	2	$\sqrt{10}$		
19	+	-2	$3\sqrt{2}$	$1/\sqrt{2}$	$1/\sqrt{2}$
20	+	0	$3\sqrt{2}$		
21	-	2	$3\sqrt{2}$		
22	+	-2	$3\sqrt{2}$	$1/\sqrt{2}$	$-1/\sqrt{2}$
23	+	0	$3\sqrt{2}$		
24	-	2	$3\sqrt{2}$		

where $\mathbf{h}$ is the vector contains the true CRs at pilot locations and $\mathbf{a}$ is the weighting vector that depends on the CR estimation method.

A. Procedure for Computing BEP

The general procedure for evaluating the BEP of an OFDM receiver with a linear channel estimate algorithms can be described as follows.

1) Derive the weighting vector $\mathbf{a}$ from the CR estimate used.
2) Evaluate the following parameters:

$$\sigma_1^2 = \frac{1}{2}E\left[|H|^2\right] \tag{55}$$

$$\sigma_2^2 = \frac{1}{2}E\left[\left|\hat{H}\right|^2\right] = \frac{1}{2}\mathbf{a}^{\mathrm{H}}\left[\mathbf{R}_{\mathbf{h}} + 2\sigma_n^2\left(\mathbf{X}\mathbf{X}^{\mathrm{H}}\right)^{-1}\right]\mathbf{a} \tag{56}$$

$$\begin{aligned}\mu_1 + i\mu_2 &= \frac{1}{2}E\left[\hat{H}H^*\right] = \frac{1}{2}\mathbf{a}^{\mathrm{H}}E\left[\mathbf{h}H^*\right] \\ &= \frac{1}{2}\mathbf{a}^{\mathrm{H}}\mathbf{r}_{\mathbf{h}H^*}\end{aligned} \tag{57}$$

$$\rho_1 = \frac{\mu_1}{\sigma_1\sigma_2} = \frac{\text{Re}\left\{\mathbf{a}^{\mathrm{H}}\mathbf{r}_{\mathbf{h}H^*}\right\}}{\sqrt{2\sigma_1^2}\sqrt{\mathbf{a}^{\mathrm{H}}\left[\mathbf{R}_{\mathbf{h}} + 2\sigma_n^2\left(\mathbf{X}\mathbf{X}^{\mathrm{H}}\right)^{-1}\right]\mathbf{a}}} \tag{58}$$

$$P_b(E) = \frac{1}{32}\sum_{k=1}^{24}\text{sgn}_k \cdot \left[1 - \frac{b_k\left[\rho_1\cos\theta_k + \rho_2\sin\theta_k\right] + \frac{a_k\sigma_2}{\sigma_1}}{\sqrt{b_k^2\left(1-\rho^2\right) + \left(b_k[\rho_1\cos\theta_k + \rho_2\sin\theta_k] + \frac{a_k\sigma_2}{\sigma_1}\right)^2 + \frac{5}{(2\cdot\overline{\gamma}_b)}}}\right] \tag{53}$$

$$\rho_2 = \frac{\mu_2}{\sigma_1\sigma_2} = \frac{\mathrm{Im}\left\{\mathbf{a}^{\mathrm{H}}\mathbf{r}_{\mathbf{h}H^*}\right\}}{\sqrt{2\sigma_1^2}\sqrt{\mathbf{a}^{\mathrm{H}}\left[\mathbf{R}_{\mathbf{h}} + 2\sigma_n^2\left(\mathbf{X}\mathbf{X}^{\mathrm{H}}\right)^{-1}\right]\mathbf{a}}} \tag{59}$$

where $\mathbf{R}_{\mathbf{h}} \triangleq E[\mathbf{h}\mathbf{h}^{\mathrm{H}}]$ and $\mathbf{r}_{\mathbf{h}H^*} \triangleq E[\mathbf{h}H^*]$.

3) Substitute ρ_1, ρ_2, σ_1 and σ_2 into a proper BEP formula.

To illustrate how the weighting vector $\mathbf{a}$ is obtained, we consider the OFDM-16QAM system. The receiver first estimates the pilot CRs by the LMMSE method (9) then compute the CR of a data location by using a polynomial interpolation, i.e.,

$$\begin{aligned}\hat{H}_n =& \mathbf{p}_n^{\mathrm{T}}\hat{\mathbf{h}}_{LMMSE} \\ =& \mathbf{p}_n^{\mathrm{T}}\tilde{\mathbf{R}}_{\mathbf{h}}\left[\tilde{\mathbf{R}}_{\mathbf{h}} + 2\tilde{\sigma}_n^2\left(\mathbf{X}\mathbf{X}^{\mathrm{H}}\right)^{-1}\right]^{-1}\hat{\mathbf{h}}_{LS}\end{aligned} \tag{60}$$

where $\mathbf{p}_n$ is the vector of the interpolating coefficients. Invoking the Lagrangian interpolation formula and equating (60) and (11), we obtain

$$\mathbf{p}_n^{\mathrm{T}} = \left[\frac{(n-L)(n-2L)}{(0-L)(0-2L)}, \frac{(n-0)(n-2L)}{(L-0)(L-2L)}, \frac{(n-0)(n-L)}{(2L-0)(2L-L)}\right]. \tag{61}$$

Therefore, the final weighting vector for the CR estimate $\hat{H}_n$ is

$$\mathbf{a}_n^{\mathrm{H}} = \mathbf{p}_n^{\mathrm{T}}\tilde{\mathbf{R}}_{\mathbf{h}}\left[\tilde{\mathbf{R}}_{\mathbf{h}} + 2\tilde{\sigma}_n^2\left(\mathbf{X}\mathbf{X}^{\mathrm{H}}\right)^{-1}\right]^{-1}. \tag{62}$$

B. Channel Correlation Functions

To evaluate the parameters, ρ_1, ρ_2, σ_2, σ_1, we need to know channel correlation functions like $\mathbf{R}_{\mathbf{h}}$ and $\mathbf{r}_{\mathbf{h}H^*}$. We consider two classes of Rayleigh channels based on Jakes model [14]. The first class has a maximum Doppler frequency f_d and an exponentially distributed delay profile with mean delay τ_d and channel correlation

$$E\left[H_{mn}H_{kl}^*\right] = \left(2\sigma_1^2\right)\frac{J_0\left(2\pi f_d(n-l)T_s\right)}{1+\left[\frac{2\pi(m-k)\tau_d}{T_s}\right]^2}\cdot\left[1 - \frac{i2\pi(m-k)\tau_d}{T_s}\right] \tag{63}$$

where $J_0(x)$ is the Bessel function of the first kind of order zero. The second class assumes an N_p-tap impulse response

$$h(t) = \sum_{k=1}^{N_p} c_k r_k(t)\delta\left(t-\tau_k\right) \tag{64}$$

where $\sum_{k=1}^{N_p} c_k^2 = 1$ and $r_k(t)$ are independent stationary complex zero-mean Gaussian processes with unit variance and τ_k is the relative delay of the kth cluster. The discrete version of this model is equivalent to a special case of the frequency-domain model of (6). The resulting channel correlation function is given by

$$\begin{aligned}E\left[H_{mn}H_{kl}^*\right] =& \left(2\sigma_1^2\right)J_0\left(2\pi f_d(n-l)T_s\right) \\ &\cdot\sum_{k=1}^{N_p} c_k^2\left\{\cos\left[2\pi(m-k)\frac{\tau_k}{T_s}\right]\right. \\ &\left.+i\sin\left[2\pi(m-k)\frac{\tau_k}{T_s}\right]\right\}.\end{aligned} \tag{65}$$

For a single-carrier narrowband channel, both (63) and (65) become

$$E\left[H_nH_l^*\right] = \left(2\sigma_1^2\right)J_0\left(2\pi f_d(n-l)T_s\right). \tag{66}$$

C. Optimal Linear CR Estimate

As has been shown before, the problem of finding the optimal linear CR estimate is equivalent to finding a weighting vector $\mathbf{a}$ that minimizes the BEP performance. Appendix C shows that, for BPSK signals, the optimal weighting vector $\mathbf{a}_{opt}$ is given by

$$\mathbf{a}_{opt} = K\left[\mathbf{R}_{\mathbf{h}} + 2\sigma_n^2\left(\mathbf{X}\mathbf{X}^{\mathrm{H}}\right)^{-1}\right]^{-1}\mathbf{r}_{\mathbf{h}H^*} \tag{67}$$

where K can be any nonzero real number. It is straightforward to show that the same conclusion holds for QPSK signals. For QAM signals, the corresponding $\mathbf{a}_{opt}$ has the same form as (67) but K is a constant that depends on the system and channel parameters. Numerical experiment has revealed that K is in the vicinity of 1 and $K = 1$ if $\mathbf{r}_{\mathbf{h}H^*}^{\mathrm{H}}\left[\mathbf{R}_{\mathbf{h}} + 2\sigma_n^2(\mathbf{X}\mathbf{X}^{\mathrm{H}})^{-1}\right]^{-1}\mathbf{r}_{\mathbf{h}H^*} = 2\sigma_1^2$.

In summary, the optimal linear CR estimate has the form of an LMMSE estimate that combines LS-estimated CRs at pilot locations by using the optimal weighting vector $\mathbf{a}_{opt}$ given by (67). The complexity of this optimal estimate is very high since we need to estimate $\mathbf{r}_{\mathbf{h}H^*}$ for each location.

D. Perfect Channel Estimation

When the perfect channel estimation is available, we have $\hat{H} = H$, $\rho_1 = 1$, $\rho_2 = 0$, $\sigma_1^2 = \sigma_2^2$ and the resulting BEP performances can serve as the lower bound for the performance of various OFDM systems in Rayleigh fading channels.

1) PSK Constellation: For this ideal case, both (31) and (32) reduce to the same BEP expression

$$P_{b,l.b.}(E) = \frac{1}{2}\left[1 - \frac{1}{\sqrt{1+\frac{1}{\bar{\gamma}_b}}}\right] \tag{68}$$

which coincides with the well-known result given by (14-3-7) of [11].

2) QAM Constellation: As for the rectangular 16-QAM system, setting $\rho_1 = 1$, $\rho_2 = 0$, and $\sigma_1 = \sigma_2$ in (53) yields

$$\begin{aligned}P_{b,l.b.}(E) =& \frac{1}{2} - \frac{3}{8}\frac{1}{\sqrt{1+\frac{5}{2\bar{\gamma}_b}}} \\ &-\frac{1}{4}\frac{1}{\sqrt{1+\frac{5}{18\bar{\gamma}_b}}} + \frac{1}{8}\frac{1}{\sqrt{1+\frac{1}{10\bar{\gamma}_b}}}.\end{aligned} \tag{69}$$

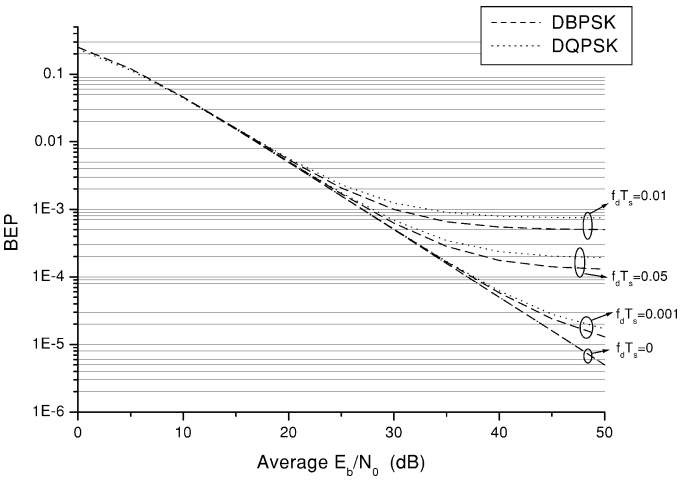

Fig. 3. BEP performance of differential BPSK and QPSK systems as functions of $\overline{\gamma}_b$ and f_dT_s.

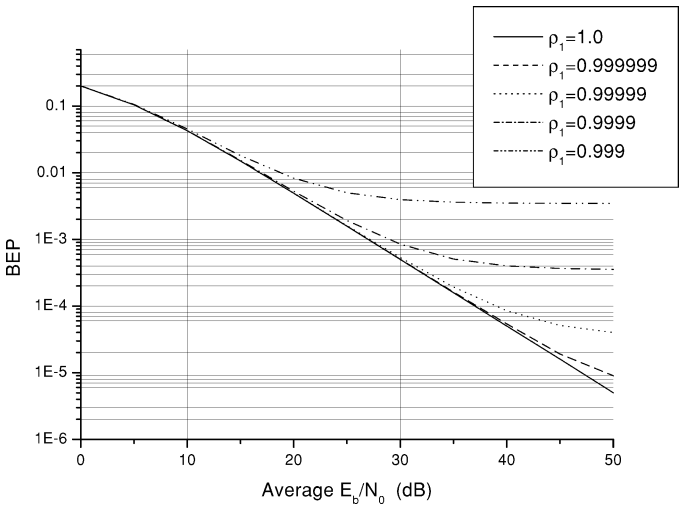

Fig. 4. BEP performance of an OFDM-16QAM system for various values of ρ_1; $\rho_2 = 0$ is assumed.

Another way to obtain this lower bound is by noticing that, as a result of $\hat{H} = H$, (26) becomes

$$\hat{X} = X + \frac{Ne^{-i\angle H}}{|H|} = X + \frac{N'}{r_1} \tag{70}$$

and the corresponding BEP becomes

$$P_{b,l.b.}(E) = \int_0^\infty P_1(r_1^2\overline{\gamma}_b|r_1)p(r_1)dr_1 \tag{71}$$

where $P_1(\cdot)$ is the BEP of the rectangular 16-QAM system in AWGN [15]

$$P_1(\overline{\gamma}_b) = \frac{3}{4}Q\left(\sqrt{\frac{4}{5}\overline{\gamma}_b}\right) + \frac{1}{2}Q\left(3\sqrt{\frac{4}{5}\overline{\gamma}_b}\right) - \frac{1}{4}Q\left(5\sqrt{\frac{4}{5}\overline{\gamma}_b}\right). \tag{72}$$

Substituting (72) into (71) gives (69).

3) Asymptotic Performance: With perfect CR information, the asymptotic BEP behaviors of various constellations converge to known results. For both BPSK and QPSK systems, (68) indicates that $P_b(E) \approx 1/(4\overline{\gamma}_b)$ for $\overline{\gamma}_b \gg 1$, while for DPSK, $P_b(E) \approx 1/(2\overline{\gamma}_b)$, according to (42) and (43). This is consistent with (14-3-13) of [11]. In the case of the rectangular 16-QAM system, (69) reveals that $P_b(E) \approx (0.4952/\overline{\gamma}_b)$ when $\overline{\gamma}_b$ is large enough.

V. Numerical Examples

This section presents some application examples of our BEP analysis. We first examine cases (Figs. 3–4) in which the BEP performance depends explicitly on some system or channel parameters, say ρ_1 or f_dT_s. Then, we consider the other cases when we must resort to the procedure given in Section IV-A in order to calculate the BEP performance.

Using (40) and (41), Fig. 3 shows the BEP performance of DPSK signals in Rayleigh fading, parameterized by f_dT_s, the normalized Doppler shift. Letting $\overline{\gamma}_b \to \infty$ in (40) and (41), we find that the corresponding BEPs approach a constant that depends on f_dT_s. The constants correspond to different f_dT_s are the error floors in the figure. The behavior of the error floor level as a function of f_dT_s is predictable as $J_0(x)$ is monotonic decreasing in the neighborhood of $x = 0$. The fact that the difference of the error floor levels of differential BPSK and QPSK systems is an increasing function of f_dT_s can also be predicted by (40) and (41).

The BEP behavior of an OFDM-16QAM system as a function of ρ_1 and $\overline{\gamma}_b$ is plotted in Fig. 4, assuming $\rho_2 = 0$ and $\sigma_1 = \sigma_2$. When $\rho_2 = 0$, ρ_1 represents the correlation between the true CR and estimated CR, higher ρ_1 not only results in smaller mean squared estimation error [see (23)] but smaller BEP as well. In a time-varying environment, smaller ρ_1 or μ_1 may be caused by higher fading rate, less frequent channel estimation (i.e., larger estimation period) and/or smaller pilot density, which, as expected, leads to higher BEP floor.

Now consider an OFDM-16QAM system whose receiver uses the LMMSE method to estimate the pilot CRs and then obtains the CRs of the data locations by a polynomial interpolation. We consider the time-varying multipath Rayleigh-fading channel based on (6). The parameter values used are $N_p = 4$, $\tau_j[n] = \tau_j$ and $h_j[n] = c_jr_j[n]$. All $r_j[n]$s are independent stationary complex zero-mean Gaussian processes with unit variance while the relative path strengths and delays are $c_j = 0.5938$, 0.7305, 0.3175, 0.1137, and $\tau_j = 0$, 0.1, 0.5, 1 μs, respectively. Assuming this receiver knows the correlation matrix $\mathbf{R_h}$ perfectly but not $\overline{\gamma}_b$, we depict the BEP performance in Fig. 5 where γ_{be} denotes the estimated $\overline{\gamma}_b$ and five pilot symbols are uniformly inserted in each block with four data symbols between two neighboring pilot symbols. These curves indicate that overestimating $\overline{\gamma}_b$ causes negligible degradation at smaller $\overline{\gamma}_b$s while underestimation leads to much greater degradation when the true $\overline{\gamma}_b$ is much larger. It is, therefore, preferred to assume a $\overline{\gamma}_b$ larger than the designed operating $\overline{\gamma}_b$.

Fig. 6 illustrates the impact of the frequency domain CR correlation on OFDM-QPSK system explicitly. Let $\mathbf{h} = (H_{0n}, H_{2n}, \ldots, H_{Ln})$ be the pilot symbol vector at

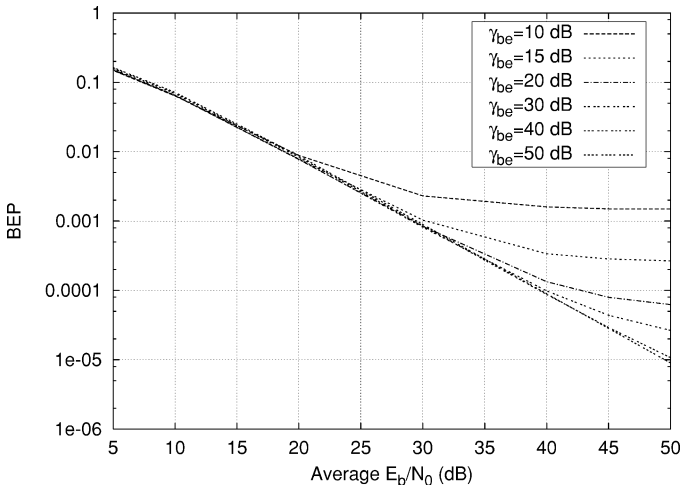

Fig. 5. BEP performance of OFDM-16QAM systems using the LMMSE method and polynomial interpolation; γ_{be} = the estimated $\overline{\gamma}_b$ and $f_d T_s = 2.76 \cdot 10^{-3}$.

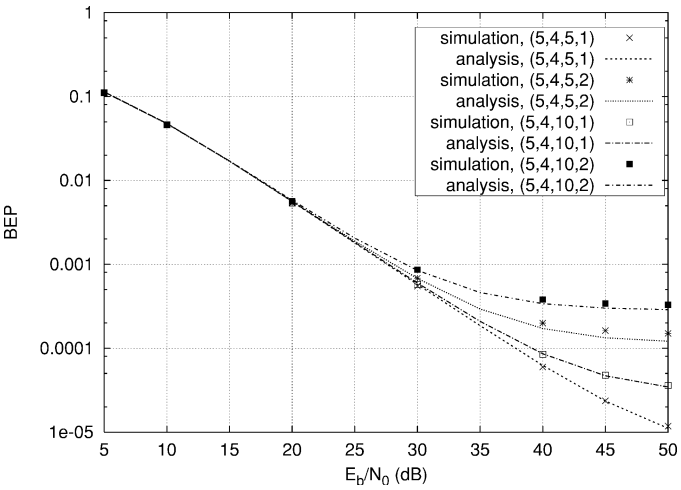

Fig. 7. BEP performance of the OFDM-16QAM system that uses the model-based channel estimate. The parameters (N_t, N_f, r_t, r_f) are defined in Fig. 1 and Section V, $f_d T_s = 2.76 \cdot 10^{-3}$.

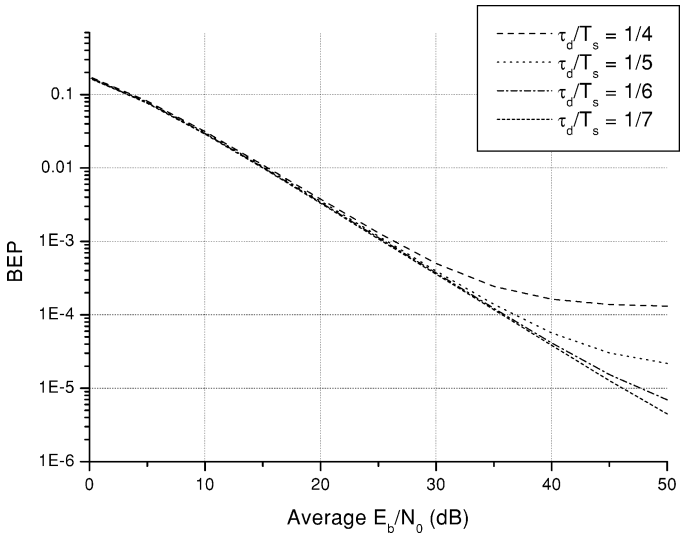

Fig. 6. BEP performance of the OFDM-QPSK system for different normalized mean channel delay τ_d/T_s which affects the channel correlation function via (73).

the nth symbol interval. The correlation values for various components of $\mathbf{h}$ can be obtained from (63) by setting $l = n$

$$E[H_{mn}H_{kn}^*] = (2\sigma_1^2)\frac{1 - \frac{i2\pi(m-k)\tau_d}{T_s}}{1 + \left[\frac{2\pi(m-k)\tau_d}{T_s}\right]^2}. \qquad (73)$$

The receiver first estimates the pilot CRs $\mathbf{h}$ by the LMMSE method, then interpolates the CRs at data locations $(H_{1n}, H_{3n}, \ldots)$ by a polynomial. Fig. 6 plots the BEP performance for different τ_d/T_ss, assuming $L = 8$. Smaller normalized mean channel delay τ_d/T_s yields larger CR correlation and smaller channel variation in frequency domain, thus reduce the channel estimation error and improve the system performance.

The BEP performance of the model-based estimate proposed in [9], with the same delay profile as the example in Fig. 5, can also be derived from our analysis. We present some typical performance in Fig. 7, where r_t, r_f are defined in Fig. 1 and N_t, N_f are the numbers of pilot symbols in the time and frequency domains per time-frequency block. The 4-tuple (N_t, N_f, r_t, r_f) thus completely specify the pilot density and the channel estimation period. As expected, increasing pilot density does indeed enhance the system BEP performance. Simulation results are also given to validate the accuracy of our analysis.

VI. Conclusion

In this work, we have presented a unified approach for analyzing the BEP performance of various OFDM systems using an arbitrary linear pilot-assisted CR estimate. Our analysis can be applied to estimate the BEP behavior of various signal constellation like QAM, PSK (BPSK, QPSK), and DPSK as long as the fading process can be modeled as a bandpass stationary zero-mean complex Gaussian process. Some of the previous known results become special cases of our general analysis, i.e., (40), (42), (43), and (68). The correctness of our analysis is verified by the fact that the system performance predicted by our analysis and computer simulation yields almost the same result. These closed-form BEP formulae enable us to derive the optimal linear CR estimate and to easily predict the influence of both the channel statistics and the CR estimation method on the system performance.

Finally, we notice that fast channel fading may cause interchannel interference (ICI) amongst subchannels. By modeling the ICI as an equivalent Gaussian noise, $\check{N}$, we can also obtain an estimation of the BEP performance by adding an equivalent variance term, $\check{\sigma}_n^2$, the variance of the ICI, to the corresponding BEP expression, if the variance can be evaluated.

Appendix A
Cross-Correlation Properties of Estimated CRs

From (12), we see that the CR estimate is a linear combination of the true CRs at pilot locations plus an independent complex Gaussian noise i.e.

$$\hat{H} = \hat{H}^{(r)} + i\hat{H}^{(i)} = H' + W = \mathbf{a}^{\mathrm{H}}\mathbf{h} + W \qquad (A.1)$$

where $\mathbf{h}=\mathbf{h}_r+i\mathbf{h}_i=[H_1,H_2,\ldots,H_L]^{\mathrm{T}}$ is the vector of the true CRs at pilot locations, $\mathbf{a}=\mathbf{a}_r+i\mathbf{a}_i=[a_1,a_2,\ldots,a_L]^{\mathrm{T}}$ is the weighted vector. In this appendix, for simplicity, we use single letter subscripts to indicate the locations of pilot symbols. The real and imaginary parts of $\hat{H}$ are denoted by $\hat{H}^{(r)}$ and $\hat{H}^{(i)}$, respectively. The real and imaginary parts of H' in (A.1) can be decomposed as $H'^{(r)}=\mathbf{a}_r^{\mathrm{T}}\mathbf{h}_r+\mathbf{a}_i^{\mathrm{T}}\mathbf{h}_i$ and $H'^{(i)}=\mathbf{a}_r^{\mathrm{T}}\mathbf{h}_i-\mathbf{a}_i^{\mathrm{T}}\mathbf{h}_r$. The stationarity assumption of the true CR process implies [12]

$$\begin{aligned}\left(E\left[\mathbf{h}_r\mathbf{h}_r^{\mathrm{T}}\right]\right)_{jk}&=E\left[H_j^{(r)}H_k^{(r)}\right]=E\left[H_j^{(i)}H_k^{(i)}\right]\\&=\left(E\left[\mathbf{h}_i\mathbf{h}_i^{\mathrm{T}}\right]\right)_{jk}\\\left(E\left[\mathbf{h}_i\mathbf{h}_r^{\mathrm{T}}\right]\right)_{jk}&=E\left[H_j^{(i)}H_k^{(r)}\right]=-E\left[H_j^{(r)}H_k^{(i)}\right]\\&=-\left(E\left[\mathbf{h}_r\mathbf{h}_i^{\mathrm{T}}\right]\right)_{jk}\end{aligned}$$

where we denote the (j,k)th entry of a matrix $\mathbf{M}$ by $(\mathbf{M})_{jk}$. Therefore, we have $E[\mathbf{h}_r\mathbf{h}_r^{\mathrm{T}}]=E[\mathbf{h}_i\mathbf{h}_i^{\mathrm{T}}]$ and $E[\mathbf{h}_i\mathbf{h}_r^{\mathrm{T}}]=-E[\mathbf{h}_r\mathbf{h}_i^{\mathrm{T}}]$, which implies

$$\mathbf{a}_r^{\mathrm{T}}E\left[\mathbf{h}_r\mathbf{h}_r^{\mathrm{T}}\right]\mathbf{a}_i=\mathbf{a}_i^{\mathrm{T}}E\left[\mathbf{h}_i\mathbf{h}_i^{\mathrm{T}}\right]\mathbf{a}_r \tag{A.2}$$

and

$$\begin{aligned}\mathbf{a}_r^{\mathrm{T}}E\left[\mathbf{h}_r\mathbf{h}_i^{\mathrm{T}}\right]\mathbf{a}_r&=\left(\mathbf{a}_r^{\mathrm{T}}E\left[\mathbf{h}_r\mathbf{h}_i^{\mathrm{T}}\right]\mathbf{a}_r\right)^{\mathrm{T}}=\mathbf{a}_r^{\mathrm{T}}E\left[\mathbf{h}_i\mathbf{h}_r^{\mathrm{T}}\right]\mathbf{a}_r\\&=-\mathbf{a}_r^{\mathrm{T}}E\left[\mathbf{h}_r\mathbf{h}_i^{\mathrm{T}}\right]\mathbf{a}_r\\\mathbf{a}_i^{\mathrm{T}}E\left[\mathbf{h}_r\mathbf{h}_i^{\mathrm{T}}\right]\mathbf{a}_i&=\left(\mathbf{a}_i^{\mathrm{T}}E\left[\mathbf{h}_r\mathbf{h}_i^{\mathrm{T}}\right]\mathbf{a}_i\right)^{\mathrm{T}}=\mathbf{a}_i^{\mathrm{T}}E\left[\mathbf{h}_i\mathbf{h}_r^{\mathrm{T}}\right]\mathbf{a}_i\\&=-\mathbf{a}_i^{\mathrm{T}}E\left[\mathbf{h}_r\mathbf{h}_i^{\mathrm{T}}\right]\mathbf{a}_i.\end{aligned}$$

Hence

$$\mathbf{a}_r^{\mathrm{T}}E\left[\mathbf{h}_r\mathbf{h}_i^{\mathrm{T}}\right]\mathbf{a}_r=0\quad\mathbf{a}_i^{\mathrm{T}}E\left[\mathbf{h}_i\mathbf{h}_r^{\mathrm{T}}\right]\mathbf{a}_i=0. \tag{A.3}$$

Equations (A.2) and (A.3) lead to

$$\begin{aligned}E[H'^{(r)}H'^{(i)}]=&\mathbf{a}_r^{\mathrm{T}}E\left[\mathbf{h}_r\mathbf{h}_i^{\mathrm{T}}\right]\mathbf{a}_r-\mathbf{a}_r^{\mathrm{T}}E\left[\mathbf{h}_r\mathbf{h}_r^{\mathrm{T}}\right]\mathbf{a}_i\\&+\mathbf{a}_i^{\mathrm{T}}E\left[\mathbf{h}_i\mathbf{h}_i^{\mathrm{T}}\right]\mathbf{a}_r-\mathbf{a}_i^{\mathrm{T}}E\left[\mathbf{h}_i\mathbf{h}_r^{\mathrm{T}}\right]\mathbf{a}_i\\=&0\\E\left[(H'^{(r)})^2\right]=&\mathbf{a}_r^{\mathrm{T}}E\left[\mathbf{h}_r\mathbf{h}_r^{\mathrm{T}}\right]\mathbf{a}_r+\mathbf{a}_r^{\mathrm{T}}E\left[\mathbf{h}_r\mathbf{h}_i^{\mathrm{T}}\right]\mathbf{a}_i\\&+\mathbf{a}_i^{\mathrm{T}}E\left[\mathbf{h}_i\mathbf{h}_r^{\mathrm{T}}\right]\mathbf{a}_r+\mathbf{a}_i^{\mathrm{T}}E\left[\mathbf{h}_i\mathbf{h}_i^{\mathrm{T}}\right]\mathbf{a}_i\\=&\mathbf{a}_r^{\mathrm{T}}E\left[\mathbf{h}_i\mathbf{h}_i^{\mathrm{T}}\right]\mathbf{a}_r-\mathbf{a}_r^{\mathrm{T}}E\left[\mathbf{h}_i\mathbf{h}_r^{\mathrm{T}}\right]\mathbf{a}_i\\&-\mathbf{a}_i^{\mathrm{T}}E\left[\mathbf{h}_r\mathbf{h}_i^{\mathrm{T}}\right]\mathbf{a}_r+\mathbf{a}_i^{\mathrm{T}}E\left[\mathbf{h}_r\mathbf{h}_r^{\mathrm{T}}\right]\mathbf{a}_i\\=&E\left[(H'^{(i)})^2\right].\end{aligned} \tag{A.4}$$

Because H' and W are independent, we have

$$E\left[\hat{H}^{(r)}\hat{H}^{(i)}\right]=0 \tag{A.5}$$

$$E\left[\hat{H}^{(r)}H^{(r)}\right]=E\left[\hat{H}^{(i)}H^{(i)}\right] \tag{A.6}$$

$$E\left[\hat{H}^{(r)}H^{(i)}\right]=-E\left[\hat{H}^{(i)}H^{(r)}\right] \tag{A.7}$$

$$E\left[\hat{H}^{(r)2}\right]=E\left[\hat{H}^{(i)2}\right]. \tag{A.8}$$

Appendix B
Derivation of an Integral Identity

We want to establish the identity

$$\begin{aligned}I\triangleq&\int_0^\infty\int_0^\infty\int_{-\pi}^{\pi}Q\left(\frac{ar_2+br_1\cos\psi}{\sigma_n}\right)\\&\cdot p(r_1,r_2,\psi)d\psi dr_1dr_2\\=&\frac{1}{2}\left[1-\frac{\left(b\rho_1+\frac{a\sigma_2}{\sigma_1}\right)}{\sqrt{b^2(1-\rho^2)+\left(b\rho_1+\frac{a\sigma_2}{\sigma_1}\right)^2+\frac{\sigma_n^2}{\sigma_1^2}}}\right]\end{aligned} \tag{B.1}$$

where $p(r_1,r_2,\psi)$ is defined by (25) and $\rho\triangleq\sqrt{\rho_1^2+\rho_2^2}$. The change of variable, $r_i'=r_i/(\sigma_i\sqrt{1-\rho^2})$, $i=1,2$, on the first line of (B.1) yields

$$\begin{aligned}I=&\frac{1-\rho^2}{2\pi}\int_0^\infty\int_0^\infty\int_{-\pi}^{\pi}Q\left(\frac{a\sigma_2r_2+b\sigma_1r_1\cos\psi}{\frac{\sigma_n}{\sqrt{1-\rho^2}}}\right)\\&\cdot\exp\left\{-\frac{1}{2}\left[r_1^2+r_2^2-2r_1r_2\left(\rho_1\cos\psi-\rho_2\sin\psi\right)\right]\right\}\\&\cdot r_1r_2\,d\psi dr_1dr_2.\end{aligned} \tag{B.2}$$

The changes of variables, $x=r_1\cos\psi+(a\sigma_2/(b\sigma_1))r_2$, $y=r_1\sin\psi$ and definition $\sigma_n'\triangleq\sigma_n/\sqrt{1-\rho^2}$, give

$$\begin{aligned}I=&\frac{1-\rho^2}{2\pi}\\&\cdot\int_0^\infty\int_{-\infty}^\infty\int_{-\infty}^\infty Q\left(\frac{b\sigma_1}{\sigma_n'}x\right)r_2\cdot\exp\left[-\frac{1}{2}\left(y+\rho_2r_2\right)^2\right]\\&\cdot\exp\left\{-\frac{1}{2}\left[\left(x-\frac{a\sigma_2}{b\sigma_1}r_2\right)^2-2\rho_1r_2\left(x-\frac{a\sigma_2}{b\sigma_1}r_2\right)\right.\right.\\&\left.\left.+\left(1-\rho_2^2\right)r_2^2\right]\right\}dydxdr_2.\end{aligned} \tag{B.3}$$

If we define $c_1\triangleq[\rho_1+(a\sigma_2/(b\sigma_1))]$ and $K\triangleq(1-\rho^2)+c_1^2$, then I can be simplified to

$$\begin{aligned}I=&\frac{1-\rho^2}{\sqrt{2\pi}}\int_0^\infty\int_{-\infty}^\infty Q\left(\frac{b\sigma_1}{\sigma_n'}x\right)\\&\cdot r_2\exp\left[-\frac{1}{2}\left(Kr_2^2-2c_1r_2x+x^2\right)\right]dxdr_2\\=&\frac{1-\rho^2}{\sqrt{2\pi}K}\int_0^\infty\int_{-\infty}^\infty Q\left(\frac{b\sigma_1}{\sigma_n'}x\right)\cdot r_2\\&\cdot\exp\left[-\frac{1}{2}\left(r_2-\frac{c_1}{\sqrt{K}}x\right)^2-\frac{1-\rho^2}{2K}x^2\right]dxdr_2\\=&\frac{1-\rho^2}{\sqrt{2\pi}K}\int_0^\infty\int_{-c_1/\sqrt{K}x}^\infty Q\left(\frac{b\sigma_1}{\sigma_n'}x\right)\left(r_2+\frac{c_1}{\sqrt{K}}x\right)\\&\cdot\exp\left[-\left(\frac{r_2^2}{2}+\frac{1-\rho^2}{2K}x^2\right)\right]dr_2dx\\&+\frac{1-\rho^2}{\sqrt{2\pi}K}\int_0^\infty\int_{-\infty}^{-c_1/\sqrt{K}x}\left[1-Q\left(\frac{b\sigma_1}{\sigma_n'}x\right)\right]\\&\cdot\left(-r_2-\frac{c_1}{\sqrt{K}}x\right)\end{aligned}$$

$$\cdot \exp\left[-\left(\frac{r_2^2}{2}+\frac{1-\rho^2}{2K}x^2\right)\right] dr_2 dx$$
$$=\frac{1-\rho^2}{\sqrt{2\pi}K}\int_0^\infty\int_{-\infty}^\infty Q\left(\frac{b\sigma_1}{\sigma_n'}x\right)\left(r_2+\frac{c_1}{\sqrt{K}}x\right)$$
$$\cdot \exp\left[-\left(\frac{r_2^2}{2}+\frac{1-\rho^2}{2K}x^2\right)\right] dr_2 dx$$
$$+\frac{1-\rho^2}{\sqrt{2\pi}K}\int_0^\infty\int_{c_1/\sqrt{K}x}^\infty \left(r_2-\frac{c_1}{\sqrt{K}}x\right)$$
$$\cdot \exp\left[-\left(\frac{r_2^2}{2}+\frac{1-\rho^2}{2K}x^2\right)\right] dr_2 dx$$
$$=I_1+I_2. \tag{B.4}$$

We now further simplify the two integrals, I_1 and I_2.

$$I_1=\frac{1-\rho^2}{\sqrt{2\pi}K}\int_0^\infty\int_{-\infty}^\infty Q\left(\frac{b\sigma_1}{\sigma_n'}x\right)\left(r_2+\frac{c_1}{\sqrt{K}}x\right)$$
$$\cdot \exp\left[-\left(\frac{r_2^2}{2}+\frac{1-\rho^2}{2K}x^2\right)\right] dr_2 dx$$
$$=\frac{(1-\rho^2)c_1}{K\sqrt{K}}\left(\frac{\sigma_n'}{b\sigma_1}\right)^2$$
$$\cdot\int_0^\infty Q\left(\operatorname{sgn}(b)\,x\right) x\exp\left[-\frac{1-\rho^2}{2K}\left(\frac{\sigma_n'}{b\sigma_1}\right)^2 x^2\right] dx$$
$$=\frac{(1-\rho^2)c_1}{K\sqrt{K}}\left(\frac{\sigma_n'}{b\sigma_1}\right)^2\frac{1}{2\frac{1-\rho^2}{K}\left(\frac{\sigma_n'}{b\sigma_1}\right)^2}$$
$$\cdot\left(1-\frac{\operatorname{sgn}(b)}{\sqrt{1+\frac{1-\rho^2}{K}\left(\frac{\sigma_n'}{b\sigma_1}\right)^2}}\right)$$
$$=\frac{c_1}{2\sqrt{K}}-\frac{c_1}{2}\frac{b}{\sqrt{b^2K+\frac{\sigma_n^2}{\sigma_1^2}}}. \tag{B.5}$$

Using the identity $K-c_1^2=1-\rho^2$, we obtain

$$I_2=\frac{1-\rho^2}{\sqrt{2\pi}K}\int_0^\infty\int_{c_1/\sqrt{K}x}^\infty\left(r_2-\frac{c_1}{\sqrt{K}}x\right)\exp\left(-\frac{1}{2}r_2^2\right)$$
$$\cdot\exp\left(-\frac{1-\rho^2}{2K}x^2\right)dr_2dx$$
$$=\frac{1-\rho^2}{\sqrt{2\pi}K}\int_0^\infty\exp\left(-\frac{1}{2}\frac{c_1^2}{K}x^2\right)\cdot\exp\left[-\frac{1}{2}\left(1-\frac{c_1^2}{K}\right)x^2\right]dx$$
$$-\frac{(1-\rho^2)c_1}{\sqrt{2\pi}K\sqrt{K}}\int_0^\infty\int_{c_1/\sqrt{K}x}^\infty x\exp\left(-\frac{1}{2}r_2^2\right)$$
$$\cdot\exp\left(-\frac{1}{2}\frac{1-\rho^2}{K}x^2\right)dr_2dx$$
$$=\frac{1-\rho^2}{2K}-\frac{(1-\rho^2)}{c_1\sqrt{K}}$$
$$\cdot\int_0^\infty Q\left(\operatorname{sgn}(c_1)x\right)\cdot x\exp\left[-\frac{1}{2}\left(\frac{K}{c_1^2}-1\right)x^2\right]dx$$
$$=\frac{1-\rho^2}{2K}-\frac{(1-\rho^2)}{c_1\sqrt{K}}\frac{1}{2\left(\frac{K}{c_1^2}-1\right)}\left[1-\frac{\operatorname{sgn}(c_1)}{\sqrt{\frac{K}{c_1^2}}}\right]$$
$$=\frac{1}{2}-\frac{c_1}{2\sqrt{K}} \tag{B.6}$$

where the sign function $\operatorname{sgn}(x)$ is defined by

$$\operatorname{sgn}(x)\triangleq\begin{cases}1, & x\geq 0\\ -1, & x<0.\end{cases} \tag{B.7}$$

Substituting (B.5) and (B.6) into (B.4), we then obtain the desired equation.

Appendix C
Optimal Linear CR Estimate

Consider an arbitrary linear pilot-assisted CR estimate of the form (12). To find the optimal CR estimate is equivalent to find the weighting vector $\mathbf{a}$ that minimizes the BEP performance. We shall only derive the optimal $\mathbf{a}$ for the BPSK system in this appendix; those for QPSK and QAM signal constellations can be obtained by analogous procedures as we can see that the BEP expressions for BPSK, QPSK, and QAM systems, (31), (32), and (53), all have similar forms.

Rewriting (31) as

$$P_b(E)=\frac{1}{2}\left[1-\frac{\mu_1}{\sqrt{\left(1+\frac{1}{\overline{\gamma}_b}\right)\sigma_1^2\sigma_2^2-\mu_2^2}}\right] \tag{C.1}$$

taking derivative with respect to $\mathbf{a}$ and setting it to zero, we obtain

$$\frac{d\mu_1}{d\mathbf{a}}\left[\left(1+\frac{1}{\overline{\gamma}_b}\right)\sigma_1^2\sigma_2^2-\mu_2^2\right]$$
$$=\frac{1}{2}\mu_1\left[\left(1+\frac{1}{\overline{\gamma}_b}\right)\sigma_1^2\frac{d\sigma_2^2}{d\mathbf{a}}-\frac{d\mu_2^2}{\mathbf{a}}\right]. \tag{C.2}$$

Substituting

$$\mu_1=0.5\operatorname{Re}\left\{\mathbf{a}^{\mathrm{H}}E[\mathbf{h}H^*]\right\}$$
$$\mu_2=0.5\operatorname{Im}\left\{\mathbf{a}^{\mathrm{H}}E[\mathbf{h}H^*]\right\}$$
$$\sigma_2^2=0.5\,\mathbf{a}^{\mathrm{H}}\left[\mathbf{R}_{\mathbf{h}}+2\sigma_n^2\left(\mathbf{X}\mathbf{X}^{\mathrm{H}}\right)^{-1}\right]\mathbf{a}$$

into (C.2), we have

$$\left[4\left(1+\frac{1}{\overline{\gamma}_b}\right)\sigma_1^2\mathbf{a}^{\mathrm{H}}\left[\mathbf{R}_{\mathbf{h}}+2\sigma_n^2\left(\mathbf{X}\mathbf{X}^{\mathrm{H}}\right)^{-1}\right]\mathbf{a}\right.$$
$$\left.-\left(\mathbf{a}^{\mathrm{H}}\mathbf{r}_{\mathbf{h}H^*}-\mathbf{r}_{\mathbf{h}H^*}^{\mathrm{H}}\mathbf{a}\right)\mathbf{r}\mathrm{H}_{\mathbf{h}}H^{*\mathbf{a}}\right]\mathbf{r}_{\mathbf{h}H^*}$$
$$=\left[2\left(1+\frac{1}{\overline{\gamma}_b}\right)\sigma_1^2\left(\mathbf{a}^{\mathrm{H}}\mathbf{r}_{\mathbf{h}H^*}+\mathbf{r}_{\mathbf{h}H^*}^{\mathrm{H}}\mathbf{a}\right)\right]$$
$$\cdot\left[\mathbf{R}_{\mathbf{h}}+2\sigma_n^2\left(\mathbf{X}\mathbf{X}^{\mathrm{H}}\right)^{-1}\right]\mathbf{a} \tag{C.3}$$

which implies

$$\mathbf{a}=K\left[\mathbf{R}_{\mathbf{h}}+2\sigma_n^2\left(\mathbf{X}\mathbf{X}^{\mathrm{H}}\right)^{-1}\right]^{-1}\mathbf{r}_{\mathbf{h}H^*} \tag{C.4}$$

where K is a scalar to be determined. Substituting (C.4) into (C.3), we have $2KK^*=(K+K^*)K$, or $K=K^*$, hence, K can be any nonzero real number. The same conclusion holds for OFDM-QPSK signals. As for OFDM-QAM signals, replacing (C.1) with (53) and following a similar approach, we find that the solution of (C.2) is still of the form of (C.4), but K now

depends on other parameters like Doppler frequency, channel delay spread and $\overline{\gamma}_b$. Numerical investigation indicates that K is usually in the vicinity of one.

REFERENCES

[1] J. A. C. Binghama, "Muticarrier modulation for data transmission: An idea whose time has come," *IEEE Commun. Mag.*, pp. 5–14, May 1990.

[2] J.-J. van de Beek, O. Edfors, M. Sandell, and S. K. Wilson, "On channel estimation in OFDM systems," in *Proc. 45th IEEE Vehicular Technology Conf.*, Chicago, IL, July 1995, pp. 815–819.

[3] O. Edfors, M. Sandell, and J.-J. van de Beek *et al.*, "OFDM channel estimation by sigular value decomposition," *IEEE Trans. Commun.*, vol. 46, pp. 931–939, July 1998.

[4] Y.(G.) Li and L. J. Cimini *et al.*, "Robust channel estimation for OFDM systems with rapid diversity fading channels," *IEEE Trans. Commun.*, vol. 46, pp. 902–915, July 1998.

[5] M. Hsieh and C. Wei, "Channel estimation for OFDM systems based on comb-type pilot arrangement in frequency selective fading channels," *IEEE Trans. Consumer Electron.*, vol. COM-46, pp. 931–939, July 1998.

[6] Y. Zhao and A. Huang, "A novel channel estimation method for OFDM mobile communication systems based on pilot signals and transform domain processing," in *Proc. IEEE 47th Vehicular Technology Conf.*, Phoenix, AZ, May 1997, pp. 2089–2093.

[7] V. Mignone and A. Morello, "CD3-OFDM: A novel demodulation scheme for fixed AHD mobile receivers," *IEEE Trans. Commun.*, vol. 44, pp. 1144–1151, Sept. 1996.

[8] M.-X. Chang and Y. T. Su, "2-D regression channel estimation for equalizing OFDM signals," in *Proc IEEE 5th Vehicular Technology Conf.*, Tokyo, May 2000, pp. 240–244.

[9] ——, "Model-based channel estimation for equalizing OFDM signals," *IEEE Trans. Commun.*, vol. 50, pp. 540–544, Apr. 2002.

[10] X. Tang, M. Alouini, and A. K. Goldsmith, "Effect of channel estimation error on M-QAM BER performance in Rayleigh fading," *IEEE Trans. Commun.*, vol. 47, pp. 1856–1864, Dec. 1999.

[11] J. G. Proakis, *Digital Communications*, 3rd ed. Englewood Cliffs, NJ: Prentice-Hall, 1995.

[12] C. W. Therrien, *Discrete Random Signals and Statistical Signal Processing*. Englewood Cliffs, NJ: Prentice-Hall, 1992.

[13] W. C. Y. Lee, *Mobile Communications Engineering*, 2nd ed. New York: McGraw-Hill, 1998.

[14] W. C. Jakes, *Microwave Mobile Communications*. New York: Wiley, 1974.

[15] M. K. Simon, S. M. Hinedi, and W. C. Lindsey, *Digital Communication Techniques*. Englewood Cliffs, NJ: Prentice-Hall, 1995.

[16] L. E. Miller, "BER expressions for differentially detected $\pi/4$ DQPSK," *IEEE Trans. Commun.*, vol. 46, pp. 71–78, Jan. 1998.

Ming-Xian Chang received the B.S. degree in electrical engineering from National Taiwan University, Taipei, Taiwan, in 1995, and the M.S. and Ph.D. degrees in communication engineering from National Chiao Tung University, Hsinchu, Taiwan, in 1997 and 2002, respectively.

He is currently an Assistant Professor in the Department of Electrical Engineering, National Cheng Kung University, Tainan, Taiwan. His current research interests include multicarrier communication systems, blind estimation, and coding theory.

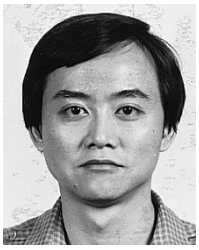

Yu T. Su (S'81–M'83) received the B.S. degree from Tatung Institute of Technology, Taipei, Taiwan, in 1974, and the M.S. and Ph.D. degrees from the University of Southern California, Los Angeles, in 1983, all in electrical engineering.

From 1983 to 1989, he was with LinCom Corporation, Los Angeles, where he was involved in the design of various measurement and digital satellite communication systems. Since September 1989, he has been with National Chiao-Tung University, Hsinchu, Taiwan, where he is presently Head of the Department of Communication Engineering. He is also affiliated with the Microelectronics and Information Systems Research Center of the same university and served as a Deputy Director from 1997 to 2000. His main research interests include communication theory and statistical signal processing.